Describing Mixture Diffusion in Microporous Materials under Conditions of Pore Saturation

Rajamani Krishna* and Jasper M. van Baten

Van't Hoff Institute for Molecular Sciences, University of Amsterdam, Science Park 904, 1098 XH Amsterdam, The Netherlands

Received: April 22, 2010; Revised Manuscript Received: June 2, 2010

In a variety of practical applications involving microporous materials such as zeolites and metal organic frameworks (MOFs), the operating conditions are such that the concentration of guest molecules within the pore space approaches saturation conditions. This situation arises, for example, in CO_2 capture processes operating at high pressures. Pore saturation is also attained in cases where micorporous materials are in contact with a bulk liquid phase. As the concentration of guest molecules within the pores approaches saturation values, the molecular jumps become increasingly correlated. In the Maxwell−Stefan (M−S) description of mixture diffusion, the increase in the correlations causes the exchange coefficient $Đ_{ij}$ to reduce in values that are significantly lower than that of the M−S diffusivities of the constituent species, $Đ_i$. We derive simplified expressions for calculation of the fluxes under this correlations dominant scenario: $Đ_i/Đ_{ij} \gg 1$. These expressions are validated by means of molecular dynamics (MD) simulations for a range of mixtures (CH_4-CO_2, CO_2-H_2, $CH_4-C_2H_6$, $CH_4-C_3H_8$, $C_2H_6-C_3H_8$, CH_4-N_2, CH_4-Ar, $Ne-Ar$, $CH_4-C_2H_6-C_3H_8$) in a variety of zeolites (MFI, BEA, ISV, FAU, NaX, NaY, LTA) and MOFs (IRMOF-1, CuBTC, MIL-53, MIL-47, Co-FA, Co(bdc)dabco, Zn(bdc)dabco).

1. Introduction

A wide variety of ordered microporous materials is used in a range of applications in storage, separation, and catalysis.[1−5] These include structures such as zeolites (crystalline aluminosilicates) and metal−organic frameworks (MOFs). In several applications, it is necessary to have a good understanding and description of the diffusion of guest molecules inside micropores.

For modeling n-component mixture diffusion, the fluxes N_i are commonly related to the chemical potential gradients$\nabla\mu_i$ by use of the Maxwell−Stefan (M−S) equations[6−16]

$$-\phi\frac{c_i}{RT}\nabla\mu_i = \sum_{\substack{j=1\\ j\neq i}}^{n}\frac{x_jN_i - x_iN_j}{Đ_{ij}} + \frac{N_i}{Đ_i};\ i = 1, 2, ..., n \tag{1}$$

where ϕ represents the fractional pore volume of the microporous crystalline material, and concentration c_i is defined in terms of moles per cubic meter of accessible pore volume. Flux N_i is defined in terms of the cross-sectional area of the crystalline framework. x_i in eq 1 is the component mole fraction of the adsorbed phase within the micropores

$$x_i = c_i/c_t;\ i = 1, 2, ..., n \tag{2}$$

$Đ_i$ characterizes species i, wall interactions in the broadest sense. $Đ_{12}$ is the exchange coefficient representing interaction between component i and component j. At the molecular level, $Đ_{ij}$ reflects how the facility for transport of species i correlates with that of species j. Conformity with the Onsager reciprocal relations prescribes

$$Đ_{ij} = Đ_{ji} \tag{3}$$

The M−S eq 1 can be rewritten to evaluate the fluxes N_i explicitly by defining a matrix $[\Delta]$

$$N_i = -\phi\sum_{j=1}^{n}\Delta_{ij}\frac{c_j}{RT}\nabla\mu_j;\ i = 1, 2, ..., n \tag{4}$$

Comparing eq 4 with eq 1, we derive the following expression for the special case of a binary mixture, that is, $n = 2$

$$[\Delta] = \begin{bmatrix} \frac{1}{Đ_1} + \frac{x_2}{Đ_{12}} & -\frac{x_1}{Đ_{12}} \\ -\frac{x_2}{Đ_{12}} & \frac{1}{Đ_2} + \frac{x_1}{Đ_{12}} \end{bmatrix}^{-1} \tag{5}$$

Formally speaking, the M−S eq 1 serves only to define the phenomenological coefficients $Đ_i$ and $Đ_{ij}$. In practice, the application of eq 1 for estimation of the fluxe N_i is based on two tenets. The first tenet is that the $Đ_i$ can be identified with the corresponding M−S diffusivity for unary diffusion, evaluated at the same total loading or occupancy θ_t

$$\theta_t = \sum_{i=1}^{n}\theta_i = \sum_{i=1}^{n}\frac{c_i}{c_{i,\mathrm{sat}}} \tag{6}$$

* Corresponding author. Tel: +31 20 6270990. Fax: + 31 20 5255604. E-mail: r.krishna@uva.nl.

10.1021/jp1036124
Published on Web 06/17/2010

where $c_{i,sat}$ is the pore concentration at saturation loadings. An exceptional circumstance manifests for CO_2-CH_4, CO_2-Ar, and CO_2-N_2 mixture diffusion in LTA, DDR, and ERI zeolites; here the preferential location of CO_2 at the window regions serves to hinder the diffusion of partner molecules, lowering its diffusivity below the pure component value.[17,18] The diffusivity of CO_2 in the mixture remains unaffected by the partner species.

The second tenet is that the exchange coefficient $Đ_{12}$ can be estimated from the pure component self-exchange coefficients $Đ_{11}$ and $Đ_{22}$ using an interpolation formula.[6−14] One such interpolation formula is based on the Vignes[19] model for diffusion in liquid mixtures

$$Đ_{12} = (Đ_{11})^{x_1}(Đ_{22})^{x_2} \quad (7)$$

The two tenets have been verified on the basis of an extensive data set of molecular dynamics (MD) simulations for a variety of mixtures containing molecules such as alkanes, CO_2, CH_4, N_2, Ar, Ne, CF_4, and He in a wide variety of microporous structures such as zeolites, metal organic framework (MOFs), and carbon nanotubes (CNTs).[7−14] Most of the validation is based on MD data for occupancies θ_t less than about 0.6. The foregoing set of equations form the basis for modeling adsorbers, reactors, and membrane permeation devices.[20−29] In the case of strong hydrogen bonding between water and alcohol molecules, both of the above-mentioned tenets break down, for example, in pervaporation applications.[30,31]

In many applications in the process industries, the operating conditions are such that the concentration of guest molecules within the pores is close to saturation conditions, that is, $\theta_t \rightarrow 1$. For example, in many CO_2 capture applications, the operating pressures are in excess of 5 MPa,[5] and consequently, the pore concentrations in adsorption and membrane technologies approach saturation conditions. In many industrial processes such as adsorptive separations of hydrocarbon isomers, the microporous materials are in contact with a bulk liquid phase mixture. In these cases, the confinement of the molecules in the micropores is high and $\theta_t \rightarrow 1$. Lettat et al.[32] provide an illustration of this by considering the liquid phase separation of hexane isomers using MFI zeolite.

The main objective of the present communication is to examine the characteristics of the matrix $[\Delta]$ under conditions of pore saturation. We derive simplified expressions for $[\Delta]$ that can be calculated solely on the basis of the pure component M−S diffusivities $Đ_i$. In particular, we aim to show that the remark made by Lettat et al.[32] "the classical adsorbed-phase diffusion models based on the Maxwell−Stefan equation cannot represent correctly multicomponent diffusion close to saturation" is unfounded. We shall demonstrate that the M−S equations provide the correct framework to derive a convenient set of expressions that hold under conditions of pore saturation.

To demonstrate the validity of the derived expressions, we have carried out MD simulations of the elements Δ_{ij} for a wide variety of binary mixtures (CH_4-CO_2, CO_2-H_2, $CH_4-C_2H_6$, $CH_4-C_3H_8$, $C_2H_6-C_3H_8$, CH_4-N_2, CH_4-Ar, $Ne-Ar$, $CH_4-C_2H_6-C_3H_8$) in different zeolites and MOFs. The chosen microporous topologies include 1D channels (AFI, MIL-47, MIL-53(Cr), Co-FA), intersecting channels (MFI, BEA, BOG, ISV, Co(bdc)dabco, Zn(bdc)dabco), large cavities with large windows (FAU, NaX, NaY, IRMOF-1, CuBTC), and cages separated by narrow windows (LTA). The elements Δ_{ij} of the matrix $[\Delta]$, required in our analysis, are directly accessible from

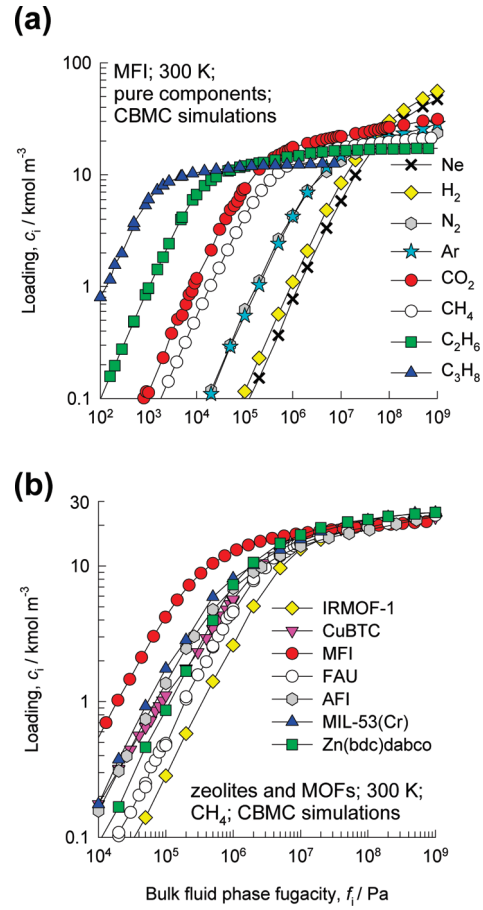

Figure 1. (a) CBMC simulations of the adsorption isotherms of (a) a variety of guest molecules in MFI zeolites at 300 K and (b) CH_4 in various zeolites and MOFs at 300 K.

MD simulations[12,13] by monitoring the individual molecular displacements in each of the three coordinate directions

$$\Delta_{ij} = \frac{1}{2}\lim_{\Delta t\rightarrow\infty}\frac{1}{n_j}\frac{1}{\Delta t}\langle(\sum_{l=1}^{n_i}(\mathbf{r}_{l,i}(t+\Delta t)-\mathbf{r}_{l,i}(t)))\cdot (\sum_{k=1}^{n_j}(\mathbf{r}_{k,j}(t+\Delta t)-\mathbf{r}_{k,j}(t)))\rangle \quad (8)$$

Additionally, the pure component M−S diffusivities $Đ_i$ for all guest−host combinations were determined. The entire database of simulation results is available in the Supporting Information accompanying this publication; this material includes details of the MD simulation methodologies, details of the microporous structures investigated (unit cell dimensions, accessible pore volume,), pore landscapes, specification of the force fields used, simulation data on the Δ_{ij}, along with the procedure for backing out the $Đ_i$, and $Đ_{ij}$ from the MD simulated Δ_{ij}.

2. Maxwell−Stefan Equations for Pore Saturation Conditions

The first task is to determine the pore saturation conditions. Figure 1a presents the configuratonal-bias Monte Carlo (CBMC) simulations of the pure component adsorption isotherms for a variety of guest molecules in MFI at 300 K. Under saturation conditions, the pore concentrations, c_i, defined in terms of the

accessible pore volume approaches values corresponding to the molar density of the guest molecule in the condensed liquid phase. From the data in Figure 1a, we obtain for C_3H_8, C_2H_6, CH_4, Ar, N_2, and CO_2 the values of $c_{i,sat}$ of 13, 17, 25, 35, 35, and 37 kmol m^{-3}, respectively. For Ne and H_2, saturation conditions are not achievable in CBMC simulations even at 1 GPa; for these two gases, we estimate $c_{i,sat} \approx 100$ kmol m^{-3}. These saturation capacity values for the variety of guest molecules will be helpful in interpreting the characteristics of the M−S diffusivities.

For any given guest molecule, an important advantage of expressing the loadings in terms of the accessible pore volumes is that these saturation capacities hold for other microporous materials as well. This is illustrated in Figure 1b, which shows the CBMC-simulated isotherms for CH_4 in various zeolites and MOFs at 300 K; all structure yield the same value $c_{i,sat} \approx 25$ kmol m^{-3}. Results that are analogous to those presented in Figure 1b are obtained for a variety of guest molecules in different microporous structures.[13,29,30,33−35]

From eq 1, we deduce that the larger the value of the M−S diffusivity $Đ_i$ with respect to exchange coefficient $Đ_{ij}$, the stronger are the consequences of correlation effects on the fluxes N_i. We may consider the ratio $Đ_i/Đ_{ij}$ as a measure of the degree of correlations. The higher this ratio, the higher is the relative contribution of the first term on the right of eq 1, relative to that of the second term on the far right. For a variety of binary mixtures, the ratios $Đ_1/Đ_{12}$ for MFI zeolite are plotted in Figure 2a as a function of the total pore concentration, $c_t = c_1 + c_2$. We note that $Đ_1/Đ_{12}$ increases by about two orders of magnitude as saturation conditions are approached. This is because unsuccessful molecular jumps and consequent revisitation of recently abandoned sites tend to increase with increasing pore occupancies.

For any mixture, the degree of correlations also depends on a variety of factors such as pore size, topology, and connectivity. This is illustrated in Figure 2b for Ne(1)−Ar(2) mixtures in a variety of zeolites and MOFs. Correlation effects are particularly strong in 1D channels such as that for AFI, MIL-47, and MIL-53. Conversely, in structures such as LTA, CHA, DDR, and ERI that consist of cages separated by narrow windows in the 3.4 to 4.2 Å size range, correlation effects are significantly lower. This is because only one molecule can hop from one cage to the next at any given time. Indeed, a good approximation to make for structures at relatively low loadings is to assume that correlations are of negligible importance, that is, $Đ_i/Đ_{ij} \rightarrow 0$. This leads to a set of uncoupled equations for the fluxes, and for binary mixtures, we get

$$\begin{bmatrix} \Delta_{11} & \Delta_{12} \\ \Delta_{21} & \Delta_{22} \end{bmatrix} = \begin{bmatrix} Đ_1 & 0 \\ 0 & Đ_2 \end{bmatrix} \tag{9}$$

MD simulations have confirmed the validity of the use of uncoupled equations for mixture diffusion in LTA, CHA, and DDR at relatively low loadings c_t.[11−14]

From the data in Figure 2a,b, we also note that $Đ_1/Đ_{12}$ values significantly exceed unity as saturation conditions are reached. For the limiting scenario where correlations are dominant, described by $Đ_i/Đ_{12} \gg 1$, we can derive the following explicit expressions for the Δ_{ij}, starting with eq 5

$$\Delta_{11} = \Delta_{12} = \frac{c_1}{\frac{c_1}{Đ_1} + \frac{c_2}{Đ_2}}; \Delta_{21} = \Delta_{22} = \frac{c_2}{\frac{c_1}{Đ_1} + \frac{c_2}{Đ_2}} \tag{10}$$

Detailed derivation of eq 10 is provided in the Supporting Information accompanying this publication. It is noteworthy that in the correlations dominant scenario, described by eq 10, the exchange coefficients do not appear. These equations imply that the elements Δ_{ij} can be calculated using the pure component $Đ_i$ without precise information on the exchange coefficient $Đ_{12}$; that is, the interpolation formula 7 is not required.

Figure 3a,b shows the MD simulated values of Δ_{ij} for $CH_4(1)-C_2H_6(2)$ mixtures, with $c_1/c_2 = 25/75$, in MFI as a function of the total pore concentration c_t. The calculations of the elements Δ_{ij} using the pure component $Đ_i$ values (open symbols) using eq 10 are denoted by the continuous solid line. We note that eq 10 provides a reasonably good quantitative prediction of the Δ_{ij} at values of c_t exceeding 15 kmol m^{-3}. The inflection in the Δ_{ij}, observed at a loading of 13 kmol m^{-3}, is to be ascribed to the corresponding inflection in the pure component M−S diffusivity of C_2H_6.

Using the saturation capacity values for CH_4 and C_2H_6 of 25 and 17 kmol m^{-3}, respectively, Figure 3c presents a plot the ratios Δ_{ij}/Δ_{ii} versus the total mixture occupancy θ_t defined by eq 6. We note that both ratios approach unity values as $\theta_t \rightarrow 1$,

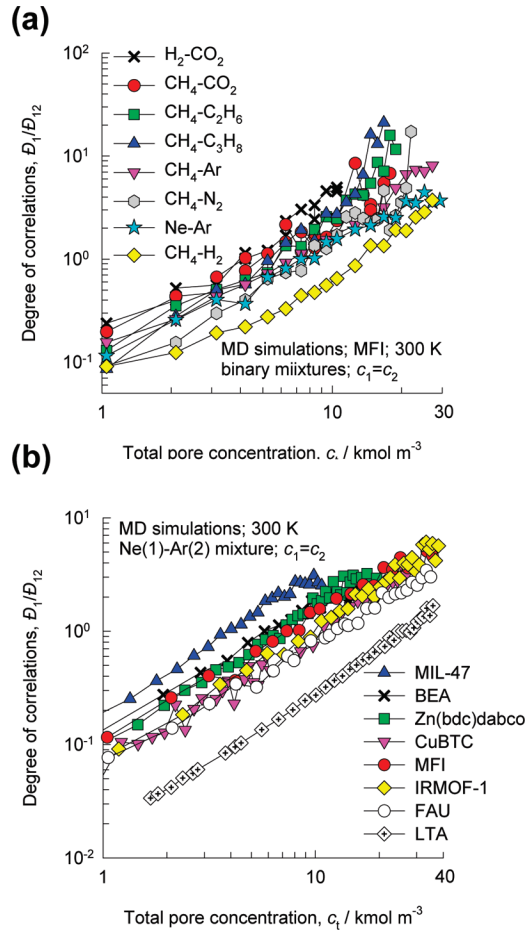

Figure 2. (a) Degree of correlations, $Đ_1/Đ_{12}$, for a variety of mixtures in MFI zeolite. (b) Degree of correlations, $Đ_1/Đ_{12}$, for Ne(1)−Ar(2) mixtures in a variety of zeolites and MOFs. The data presented here are backed out from the MD-simulated Δ_{ij} using the procedure described in the Supporting Information.

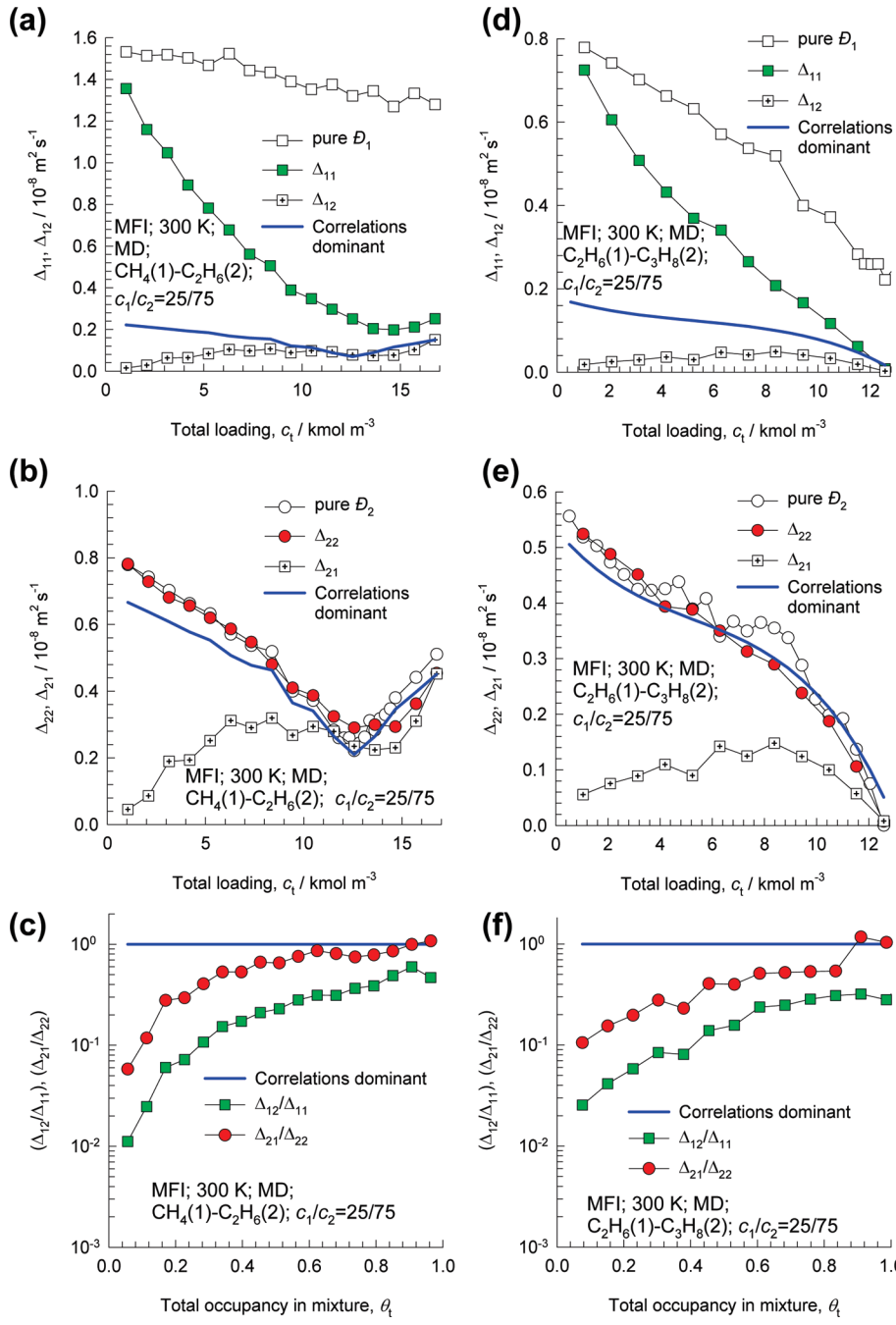

Figure 3. MD-simulated values (filled symbols) of Δ_{ij} for binary mixtures (a,b) $CH_4(1)-C_2H_6(2)$ and (c,d) $C_2H_6(1)-C_3H_8(2)$ in MFI at 300 K as a function of the total pore concentration $c_t = c_1 + c_2$. Also shown with open symbols are MD-simulated pure components $Đ_1$ and $Đ_2$. The pore concentration ratio, $c_1/c_2 = 25/75$. The continuous lines are the predictions of eq 10 using the pure component $Đ_1$ and $Đ_2$ from MD simulations.

corresponding to saturation, indicating a significant increase in the degree of diffusional coupling.

Exactly analogous results are obtained for $C_2H_6(1)-C_3H_8(2)$ mixtures in MFI; see Figure 3d−f. In this case, saturation capacity values for C_2H_6 and C_3H_8 of 17 and 13 kmol m^{-3} are used to determine the mixture occupancy θ_t.

For both alkane mixtures considered in Figures 3, we note that the diagonal element of the tardier species, Δ_{22}, equals the calculations of the correlations dominant scenario over the entire composition range and not just near saturation concentrations. This is a physically rational result. Correlations tend to slow down the more mobile species, and in the limit of correlations being dominant, the calculations using eq 10 tend to equal the value of the diffusivity of the tardier species.

For the special case of an equimolar binary mixture, that is, $c_1 = c_2$, eq 10 further simplifies to yield

$$\Delta_{11} = \Delta_{12} = \Delta_{22} = \Delta_{21} = \frac{1}{\frac{1}{Đ_1} + \frac{1}{Đ_2}} \qquad (11)$$

This indicates that all four elements of the matrix $[\Delta]$ are equal to one another, and there is just one characteristic diffusivity in the mixture.

Figure 4 presents data on MD simulated values of Δ_{ij} for various equimolar binary mixtures ($c_1 = c_2$) in a variety of zeolites and MOFs, as a function of the total pore concentration

$c_t = c_1 + c_2$. As saturation is approached, all Δ_{ij} appear to converge to the same value. The continuous lines are the predictions of eq 11 using the pure component $Đ_1$ and $Đ_2$ from MD simulations. In all cases, the Δ_{ij} values are seen to converge toward one another, and eq 11 is a reasonably good representation of Δ_{ij} of this limiting value. The Supporting Information provides further evidence of the validity of eqs 10 and 11 for a wide variety of mixtures in different microporous host structures.

In this context, it is worth mentioning that for mixture diffusion in CNTs, MD simulations have shown that eq 11 holds over the entire range of pore concentrations and not just near saturation conditions.[10,12,36,37]

For the general case of an n-component mixture, the expressions for Δ_{ij} in the correlations dominant scenario are

$$\Delta_{ij} = \frac{c_i}{\frac{c_1}{Đ_1} + \frac{c_2}{Đ_2} + ... + \frac{c_n}{Đ_n}}; i,j = 1,2,...,n \quad (12)$$

Equation 12 signifies that each of the ratios Δ_{ij}/Δ_{ii} equals unity in the correlations-dominant scenario. Figure 5 presents data for the ratios Δ_{ij}/Δ_{ii} for equimolar $CH_4(1)-C_2H_6(2)-C_3H_8(3)$ mixtures in MFI. All ratios Δ_{ij}/Δ_{ii} are seen to approach unity as saturation conditions are approached.

Lettat et al.[32] have adopted a different approach to describe diffusion under saturation conditions. They assume the exchange coefficient $Đ_{ij}$ to have infinitely large values. Coupling effects are accounted for by introducing additional constraints.

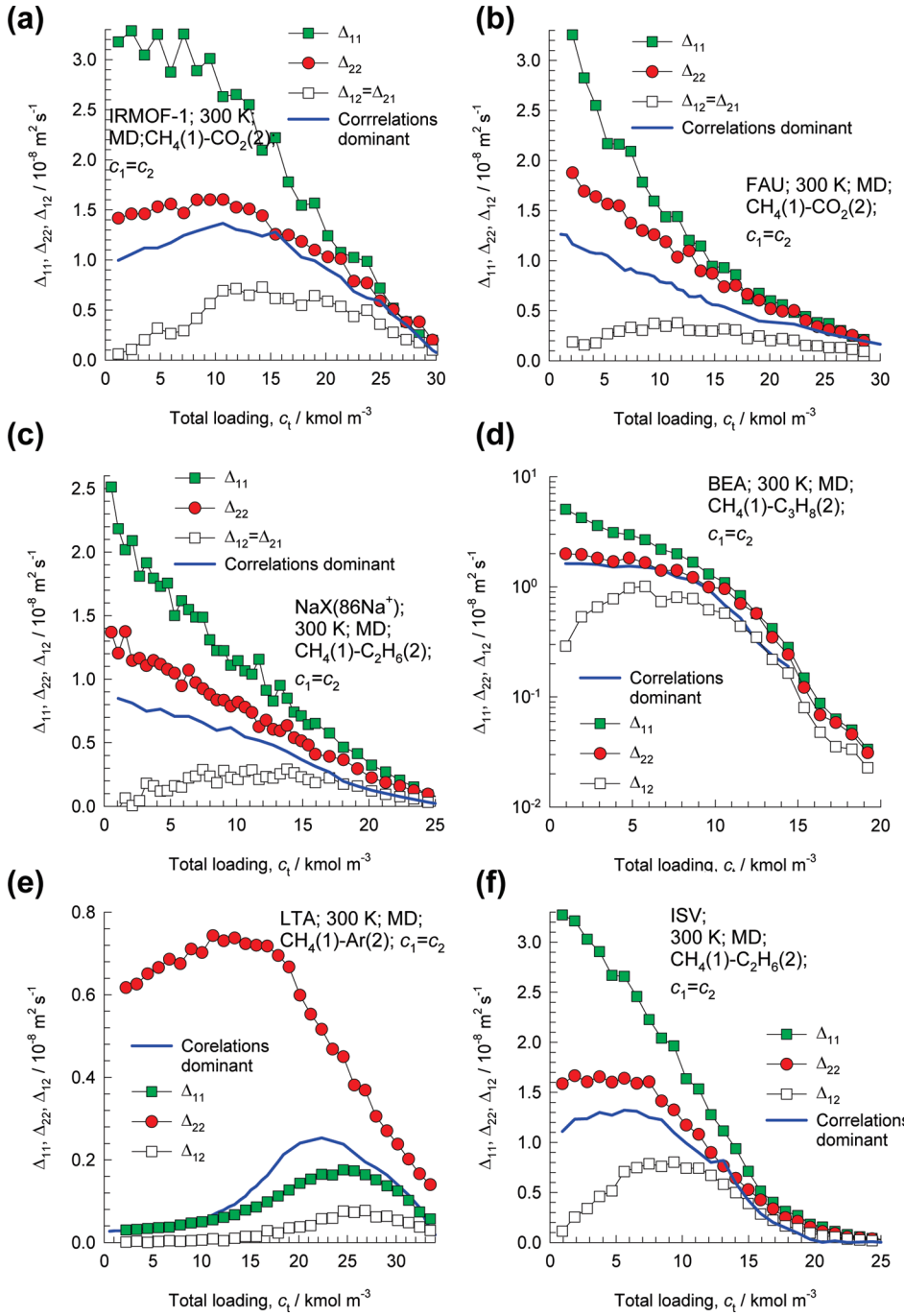

Figure 4. MD-simulated values of Δ_{ij} for various equimolar binary mixtures ($c_1 = c_2$) in a variety of zeolites and MOFs as a function of the total pore concentration $c_t = c_1 + c_2$. The continuous lines are the predictions of eq 11 using the pure component $Đ_1$ and $Đ_2$ from MD simulations.

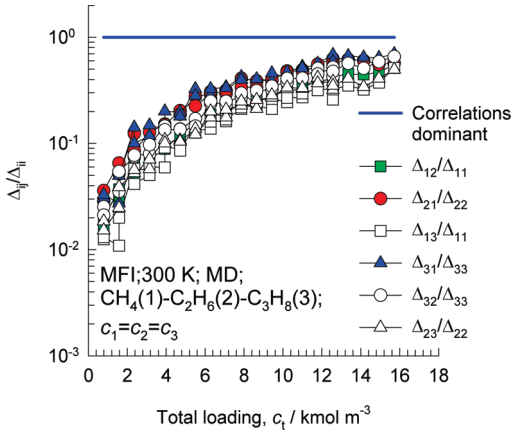

Figure 5. MD simulated values of the ratios Δ_{ij}/Δ_{ii} for equimolar ($c_1 = c_2 = c_3$) ternary $CH_4(1)-C_2H_6(2)-C_3H_8(3)$, mixtures in MFI as a function of the total pore concentration c_t.

3. Comparison of Δ_{ij} for Different Microporous Structures

Let us now compare the calculations of Δ_{ij} for equimolar binary mixture diffusion, following eq 11, in different microporous structures. Figure 6a presents calculations for CH_4-CO_2 mixtures. The hierarchy of values is largely dictated by the degree of confinement of guest molecules.[13,14] The larger the pore size, the smaller the degree of confinement, and this leads to a higher value of Δ_{ij}. This trend is exemplified by MIL-53(Cr) > FAU > MFI, with characteristic pore dimensions of 8.5, 7.4, and 5.7 Å. For the same FAU pore topology, we find that the Δ_{ij} values decrease with increasing number of cations, that is, FAU (0 Na^+) > NaY (54 Na^+) > NaX (86 Na^+). The reason for this is that the adsorption strength increases with increasing number of cations, and this increases the "stricking tendency" that contributes to a lower mobility within the pores.[14]

As pore saturation conditions are approached, $c_{t,sat} \approx 30$ kmol m^{-3}, the Δ_{ij} tend to reduce sharply. For comparison purposes, we have also shown the M−S diffusivity of the CH_4-CO_2 mixture in the fluid phase, $Đ_{12,fl}$. The asymptotic drop in the Δ_{ij} values corresponds with that of $Đ_{12,fl}$. For any given microporous structure, the Δ_{ij} at $c_{t,sat}$ remains lower than the $Đ_{12,fl}$ because of the influence of guest−host interactions. The more open the structure, the closer Δ_{ij} is to $Đ_{12,fl}$. Conversely, in more constrained pores, the Δ_{ij} can be lower than $Đ_{12,fl}$ by about an order of magnitude. The liquid phase diffusivity value, multiplied by an appropriate factor lower than unity, provides a reasonable starting point for rough estimation purposes.

A similar trend to that observed for CH_4-CO_2 mixtures holds for $CH_4-C_2H_6$, $CH_4-C_3H_8$, and CH_4-Ar mixtures. (See Figure 6b−d.)

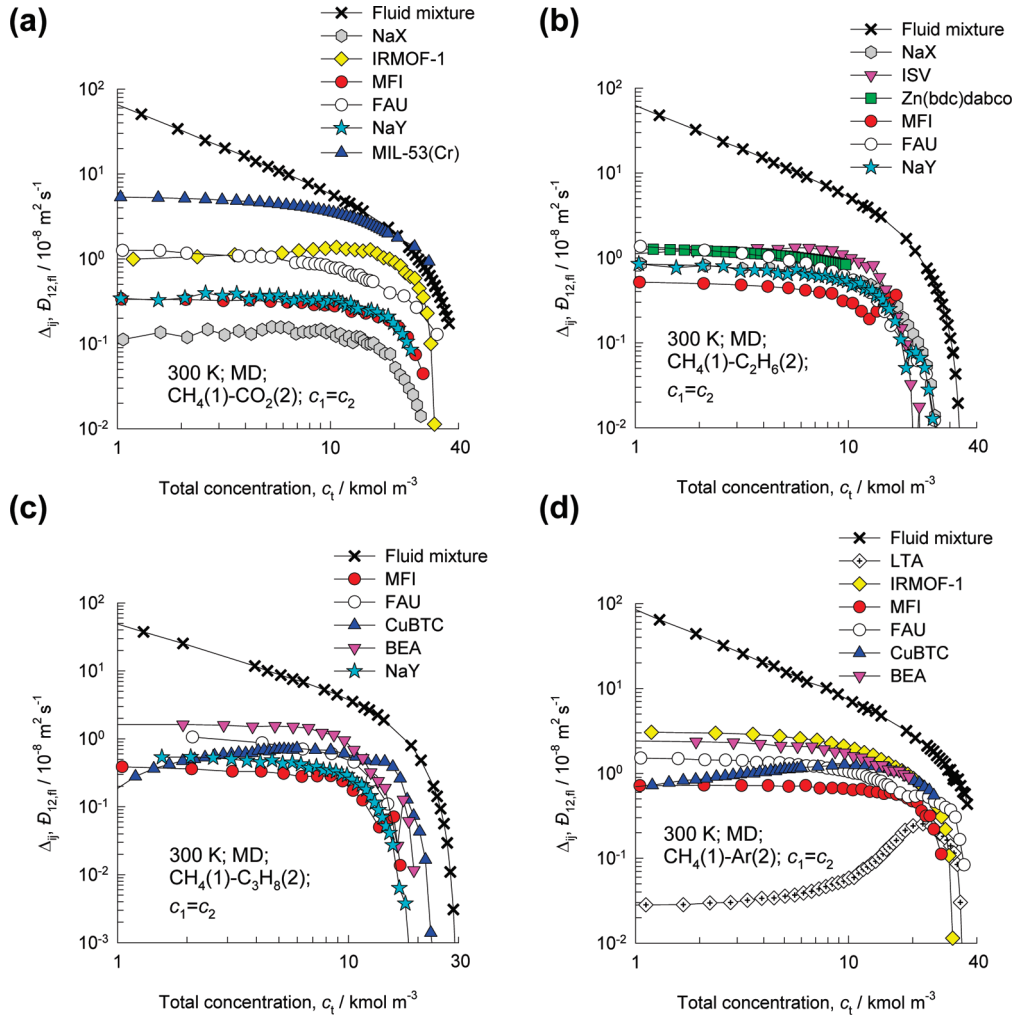

Figure 6. Calculations of Δ_{ij} using eq 11 for equimolar binary mixtures ($c_1 = c_2$) of (a) $CH_4(1)-CO_2(2)$, (b) $CH_4(1)-C_2H_6(2)$, (c) $CH_4(1)-C_3H_8(2)$, and (d) $CH_4(1)-Ar(2)$ in a variety of zeolites and MOFs as a function of the total pore concentration $c_t = c_1 + c_2$. Also shown are the MD simulated values of the binary M−S diffusivity for an equimolar fluid mixture, $Đ_{12,fl}$, at the corresponding value of concentration c_t.

4. Conclusions

Assuming a scenario in which diffusional correlations are dominant, we have derived simplified expressions given by eqs 10 and 12 for estimating the elements of the matrix [Δ] for conditions corresponding to saturation within the pores. With the aid of an extensive database of MD simulations for a wide variety of binary mixtures in several microporous host structures, the correlations-dominant scenario has been shown to hold as a good approximation as the mixture occupancy approach θ_t approaches unity. The developed expressions are particularly convenient to use in practice because there is no need to estimate the exchange coefficient $Đ_{ij}$.

Acknowledgment. R.K. acknowledges the grant of a TOP subsidy from The Netherlands Foundation for Fundamental Research (NWO-CW) for intensification of reactors.

Notation

c_i	pore concentration of species i, mol m^{-3}
$c_{i,sat}$	saturation capacity of species i, mol m^{-3}
c_t	total pore concentration in mixture, mol m^{-3}
$Đ_i$	M−S diffusivity of species i, m^2 s^{-1}
$Đ_{ij}$	M−S exchange coefficient, m^2 s^{-1}
$Đ_{ij,fl}$	M−S diffusivity in binary i-j fluid mixture, m^2 s^{-1}
f_i	fluid phase fugacity of species i, Pa
n	number of components in mixture, dimensionless
n_i	number of molecules of species i in simulation box, dimensionless
N_i	molar flux of species i defined in terms of the cross-sectional area of the crystalline framework, mol m^{-2} s^{-1}
$\mathbf{r}_{l,i}(t)$	position vector for molecule l of species i at any time t, m
R	gas constant, 8.314 J mol^{-1} K^{-1}
t	time, s
T	absolute temperature, K
x_i	mole fraction of species i based on loading within pore, dimensionless

Greek Letters

Δ_{ij}	diffusivities defined by eq 4, m^2 s^{-1}
ϕ	fractional pore volume of microporous material, dimensionless
μ_i	molar chemical potential, J mol^{-1}
θ_i	fractional occupancy of species i, dimensionless
θ_t	total occupancy in mixture, dimensionless

Subscripts

i	referring to component i
fl	referring to fluid phase
sat	referring to saturation conditions
t	referring to total mixture

Supporting Information Available: Detailed derivations of the expressions for correlations dominant scenario using the Maxwell−Stefan equations. The pore landscapes and structural details of a variety of microporous structures (zeolites, MOFs) referred to in this article along with force fields and simulation methods. Simulation results for the elements Δ_{ij} for different guest−host combinations along with comparison with the predictions of eq 12 using pure component data on $Đ_i$.

Video animations of mixture diffusion in MFI, AFI, and LTA; these give a visual appreciation of mixture diffusion under conditions close to saturation loadings.

This material is available free of charge via the Internet at http://pubs.acs.org.

References and Notes

(1) Czaja, A. U.; Trukhan, N.; Müller, U. *Chem. Soc. Rev.* **2009**, *38*, 1284–1293.
(2) Li, J. R.; Kuppler, R. J.; Zhou, H. C. *Chem. Soc. Rev.* **2009**, *38*, 1477–1504.
(3) Férey, G.; Serre, C. *Chem. Soc. Rev.* **2009**, *38*, 1380–1399.
(4) Gascon, J.; Kapteijn, F. *Angew. Chem., Int. Ed.* **2010**, *49*, 1530–1532.
(5) D'Alessandro, D. M.; Smit, B.; Long, J. R. *Angew. Chem., Int. Ed.*, in press. http://dx.doi.org/10.1002/anie.201000431.
(6) Kapteijn, F.; Moulijn, J. A.; Krishna, R. *Chem. Eng. Sci.* **2000**, *55*, 2923–2930.
(7) Skoulidas, A. I.; Sholl, D. S.; Krishna, R. *Langmuir* **2003**, *19*, 7977–7988.
(8) Chempath, S.; Krishna, R.; Snurr, R. Q. *J. Phys. Chem. B* **2004**, *108*, 13481–13491.
(9) Krishna, R.; van Baten, J. M. *J. Phys. Chem. B* **2005**, *109*, 6386–6396.
(10) Krishna, R.; van Baten, J. M. *Ind. Eng. Chem. Res.* **2006**, *45*, 2084–2093.
(11) Krishna, R.; van Baten, J. M. *Microporous Mesoporous Mater.* **2008**, *109*, 91–108.
(12) Krishna, R.; van Baten, J. M. *Chem. Eng. Sci.* **2008**, *63*, 3120–3140.
(13) Krishna, R.; van Baten, J. M. *Chem. Eng. Sci.* **2009**, *64*, 3159–3178.
(14) Krishna, R. *J. Phys. Chem. C* **2009**, *113*, 19756–19781.
(15) Wang, Y.; LeVan, M. D. *J. Phys. Chem. B* **2008**, *112*, 8600–8604.
(16) Dubbeldam, D.; Snurr, R. Q. *Mol. Simul.* **2007**, *33*, 15–30.
(17) Krishna, R.; van Baten, J. M. *Chem. Phys. Lett.* **2007**, *446*, 344–349.
(18) Krishna, R.; van Baten, J. M. *Sep. Purif. Technol.* **2008**, *61*, 414–423.
(19) Vignes, A. *Ind. Eng. Chem. Fundam.* **1966**, *5*, 189–199.
(20) Krishna, R.; Baur, R. *Sep. Purif. Technol.* **2003**, *33*, 213–254.
(21) van de Graaf, J. M.; Kapteijn, F.; Moulijn, J. A. *AIChE J.* **1999**, *45*, 497–511.
(22) Hansen, N.; Krishna, R.; van Baten, J. M.; Bell, A. T.; Keil, F. J. *J. Phys. Chem. C* **2009**, *113*, 235–246.
(23) Hansen, N.; Krishna, R.; van Baten, J. M.; Bell, A. T.; Keil, F. J. *Chem. Eng. Sci.* **2010**, *65*, 2472–2480.
(24) Li, S.; Falconer, J. L.; Noble, R. D.; Krishna, R. *J. Phys. Chem. C* **2007**, *111*, 5075–5082.
(25) Krishna, R.; van Baten, J. M.; García-Pérez, E.; Calero, S. *Ind. Eng. Chem. Res.* **2007**, *46*, 2974–2986.
(26) Krishna, R.; Li, S.; van Baten, J. M.; Falconer, J. L.; Noble, R. D. *Sep. Purif. Technol.* **2008**, *60*, 230–236.
(27) Gavalas, G. R. *Ind. Eng. Chem. Res.* **2008**, *47*, 5797–5811.
(28) Wang, Y.; LeVan, M. D. *Ind. Eng. Chem. Res.* **2007**, *46*, 2141–2154.
(29) Krishna, R.; van Baten, J. M. *J. Membr. Sci.*, in press. http://dx.doi.org/10.1016/j.memsci.2010.05.032.
(30) Krishna, R.; van Baten, J. M. *Langmuir*, published online April 22, http://dx.doi.org/10.1021/la100737c.
(31) Krishna, R.; van Baten, J. M. *J. Membr. Sci.*, in press. http://dx.doi.org/10.1016/j.memsci.2010.05.049.
(32) Lettat, K.; Jolimaître, E.; Tayakout, M.; Tondeur, D. *AIChE J.*, published online April 5, http://dx.doi.org/10.1002/aic.12268.
(33) Krishna, R.; van Baten, J. M. *Langmuir* **2010**, *26*, 3981–3992.
(34) Krishna, R.; van Baten, J. M. *Langmuir* **2010**, *26*, 2975–2978.
(35) Krishna, R.; van Baten, J. M. *Langmuir* **2010**, *26*, 8450–8463.
(36) Chen, H. B.; Sholl, D. S. *J. Am. Chem. Soc.* **2004**, *126*, 7778–7779.
(37) Arora, G.; Sandler, S. I. *J. Chem. Phys.* **2006**, *124*, 084702.

JP1036124